Materials Science & Engineering B 251 (2019) 114468

Contents lists available at ScienceDirect

Materials Science & Engineering B

journal homepage: www.elsevier.com/locate/mseb

Solid polymer electrolytes based on poly(vinyl alcohol) incorporated with sodium salt and ionic liquid for electrical double layer capacitor

N. Farah[a], H.M. Ng[a], Arshid Numan[b,c], Chiam-Wen Liew[d], N.A.A. Latip[a], K. Ramesh[a], S. Ramesh[a,*]

[a] Centre for Ionics University of Malaya, Department of Physics, Faculty of Science, University of Malaya, 50603 Kuala Lumpur, Malaysia
[b] State Key Laboratory of ASIC and System, SIST, Fudan University, 200433 Shanghai, China
[c] Graphene & Advance 2D Materials Research Group, School of Science and Technology, Sunway University, No. 5, Jalan University, Bandar Sunway, 47500 Subang Jaya, Selangor, Malaysia
[d] Department of Physical Science, Faculty of Applied Sciences, Tunku Abdul Rahman University College, Jalan Genting Kelang, Setapak, 53300 Kuala Lumpur, Malaysia

ARTICLE INFO

Keywords:
Solid polymer electrolyte
Electrical double layer capacitor
Sodium trifluoromethanesulfonate
Ionic liquid

ABSTRACT

Solid polymer electrolyte (SPE) based on poly(vinyl alcohol) (PVA) as a host polymer, sodium trifluoromethanesulfonate (NaTf) salt, and 1-butyl-3-methylimidazolium bromide (BmImBr) ionic liquid is fabricated using solution casting technique. The ionic conductivity, crystallinity, composition and thermal stability were characterized by electrochemical impedance spectroscopy (EIS), X-ray diffraction (XRD), Fourier transform infrared spectroscopy (FTIR) and thermogravimetric analysis (TGA), respectively. The optimum ratio between PVA and NaTf salt to obtain highest ionic conductivity was found to be as 60:40. The inclusion of BmImBr ionic liquid into the optimized PVA-based SPE significantly enhanced the ionic conductivity. XRD pattern indicated the successful dissolution of NaTf salt and complexation of BmImBr ionic liquid in the host polymer which has also been confirmed by FTIR spectra. The thermally stable SPE is suitable for electrical double layer capacitor (EDLC) application. The electrochemical studies of GPE for EDLC showed promising performance producing specific capacitance of 16.32 F g^{-1}.

1. Introduction

The imminent depletion of fossil fuels and large scale production of greenhouse gases due to their rapid consumption are the alarming environmental concerns. These issues have stimulated the search for green and alternative energy resources as well as energy storage devices [1,2]. Among the family of energy storage devices, supercapacitor is the new generation energy storage device that has drawn considerable interest owing to its high power density compared to batteries and high energy density compared to conventional capacitors [3,4]. Supercapacitor can be classified in to two types on the basis of charge storage mechanism. First type is pseudocapacitor, which uses faradaic reactions to store charges while second type is electrical double layer capacitor (EDLC), where electric energy is stored via reverse adsorption of ions on electrode and electrolyte interface [5]. Unlike to pseudocapacitor, EDLC works on the reversible adsorption of ions without involving any faradaic reactions. Therefore, the life cycle of EDLC is much higher compared to pesoudocapacitor [6]. In addition to this, pseudocapacitors usually uses liquid electrolyte which result in bulky and heavy device. Moreover, the risk of using harmful and corrosive liquid electrolyte can cause safety issues [7]. However, EDLC employs solid polymer electrolyte (SPE) membranes which offer wide operating temperature range, low volatility, high energy density, no new technology requirements and negligible vapor pressure [8]. Due to their thin and elastic polymeric matrix, solid, flexible and even bendable EDLC can be fabricated in variety of shapes. SPE plays major role in the operation of EDLC and it is synthesized by the complexation of the salt of alkali metals with host polymer [9]. PVA is one of the most promising polymers that have great potential to be used as host polymer due to its unique structure. It consists of carbon backbone chain with hydroxyl groups attached on it [10]. The hydroxyl groups can favor the bond formation which can facilitate in the complexation of salt, ionic liquid and nanofillers. The high mechanical strength, non-toxicity, biocompatibility, high permeability, biodegradable and facile preparation are the fascinating features of PVA which makes it suitable to be used as host polymer in energy storage applications [11,12].

Nonetheless, high crystallinity of PVA caused SPE to have low ionic conductivity. The conductivity of PVA can be enhanced by introduction

* Corresponding author.
E-mail address: ramesh@um.edu.my (S. Ramesh).

https://doi.org/10.1016/j.mseb.2019.114468
Received 16 November 2017; Received in revised form 8 September 2019; Accepted 9 November 2019
Available online 18 November 2019
0921-5107/

of salt, which can provide ions for the conduction. Sodium salts are emerging as better choice for energy storage applications compared to lithium salt because sodium raw material is much cheaper (30–40 times) and its reserves are abundant and can be easily obtained compared to lithium [13]. The ions of sodium suffer from sluggish kinetics due to their large size. This can be compensated by the addition of additives such as ionic liquid, plasticizer and filler. High ion content, better thermal stability, non-volatile, non-flammable, low viscosity, wider electrochemical operating potential window and environmentally friendly are the characteristics of ionic liquid that play major role in electrochemical applications [14]. Similar to plasticizer, an ionic liquid can induce the formation of amorphous phase by the voluminous cations to create "free-volume" which is favorable for ion diffusion [15,16].

Based on above discussion, SPE composed on PVA host polymer, NaTf salt and 1-butyl-3-methylimidazolium bromide (BmImBr) ionic liquid is synthesized by solution casting method. The prepared SPE is combined with carbon-based electrodes to fabricate EDLC. The mixture of activated carbon and carbon nanotubes (CNTs) was used to fabricate the electrodes. Activated carbon provide large specific surface area (1000–2500 m^2g^{-1}). CNTs were used to provide mesoporous structure to overcome the limitation of activated carbon that has high microporosity which limit the charge carriers to pass through the activated carbon to increase ion absorption [17,18]. The electrochemical performance of the fabricated EDLC using ionic liquid-added SPEs was analyzed by electrochemical impedance spectroscopy (EIS), cyclic voltammetry (CV) and galvanostatic charge discharge (GCD).

2. Experimental

2.1. Materials

Poly(vinyl alcohol) (PVA) and sodium trifluoromethanesulfonate (NaTf) were obtained from Sigma-Aldrich and 1-butyl-3-methylimidazolium bromide (BmImBr) was obtained from Merck. Activated carbon (AC), carbon black, carbon nanotubes (CNTs), poly(vinylidene fluoride) (PVdF) and 1-methyl-2-pyrrolidone used to prepare carbon slurry were obtained from Sigma-Aldrich. All the chemical used were of analytical grade. Deionized water was used throughout experiment.

2.2. Preparation of solid polymer electrolyte (SPE)

The preparation of PVA-based SPEs involve solution casting method. The weight ratio of PVA and $NaCF_3SO_3$ (NaTf) was varied which is summarized in Table 1. Both the materials were dissolved in 25 mL deionized water under constant stirring. The mixture was continuously stirred for 4 h at 120 °C. Then solution was poured into a glass petri dish and dried overnight at 40 °C. The free standing thin film was obtained and the conductivity was analyzed by EIS.

The highest conducting SPE based on PVA and NaTf system was then incorporated with BmImBr ionic liquid. The contents of BmImBr were varied according to Table 2, in order to get best SPE. The preparation method of SPE incorporated with BmImBr ionic liquid followed the same procedure as described above.

Table 1
The composition of ionic liquid-free SPEs based on PVA and NaTf.

Sample	Weight ratio (PVA:NaTf)	PVA (g)	NaTf (g)
PVA90	90:10	0.9	0.1
PVA80	80:20	0.8	0.2
PVA70	70:30	0.7	0.3
PVA60	60:40	0.6	0.4

Table 2
The composition of BmImBr ionic liquid-added SPEs.

Sample	PVA60: BmImBr	PVA (g)	NaTf (g)	BmImBr (g)
IL-0.1	1: 0.1	0.6	0.4	0.1
IL-0.2	1: 0.2	0.6	0.4	0.2
IL-0.3	1: 0.3	0.6	0.4	0.3
IL-0.4	1: 0.4	0.6	0.4	0.4
IL-0.5	1: 0.5	0.6	0.4	0.5
IL-0.6	1: 0.6	0.6	0.4	0.6

2.3. Characterization of solid polymer electrolyte

The conductivity studies through EIS was performed by using HIOKI 3532-50 LCR HiTESTER impedance analyzer at room temperature. The SPE sample was placed between two stainless steel blocking electrodes. The frequency range was fixed from 50 Hz to 5 MHz.

The ionic conductivity from EIS was calculated by Eq. (1).

$$\sigma = \frac{l}{R_b A} \tag{1}$$

where l is thickness of SPE in cm; R_b is bulk resistance of SPE in ohm (Ω) and A is the surface area (cm^2) of blocking electrodes. The temperature dependent ionic conductivity studies of SPEs were carried out in a temperature range of 30–120 °C at interval of 10 °C. At each temperature, the sample was allowed to stabilize for about 30 min before the measurement was taken.

The thermal stability of SPE films were analyzed by TGA using thermogravimetric analysis TGA Q500 V20.13 Build 39 which is heated from 30 to 800 °C. The complexation in polymer matrix can be observed by conducting FTIR spectroscopy using Thermoscientific Nicolet i510 FTIR spectrometer in the range of 650–4000 cm^{-1} with a resolution of 1 cm^{-1} in transmittance mode. The crystallinity of the SPE films was analyzed by XRD spectra using Olympus BTX benchtop X–ray diffraction System in a 2θ angle from 5° to 55°.

2.4. Fabrication and characterization of electrical double layer capacitors (EDLC)

In order to fabricate the electrode, carbon slurry was prepared by mixing 80 wt% activated carbon, 5 wt% carbon black, 5 wt% carbon nanotubes, 10 wt% PVdF as binder and NMP as a solvent. Above mixture was stirred for few hours at ambient temperature to obtain uniform slurry. This slurry was spin coated on aluminum at 2500 rpm for 30 s foil substrate and dried in a vacuum oven for 7 h at 70 °C.

Supercapacitor cell was fabricated by dropping electrolyte solution on the carbon coated aluminum electrodes followed by spin coating for 60 s at 2000 rpm. This step was repeated for few times until the electrolyte solution absorbed into the electrode surface. Both electrodes were combined and dried over night at 40 °C. The electrochemical performance of fabricated EDLC was then analyzed using CV, GCD and EIS.

3. Results and discussion

3.1. Electrochemical impedance spectroscopy (EIS)

The optimum amount of NaTf in the PVA host polymer was obtained through ionic conductivity of the SPE films. The ionic conductivity of SPEs at room temperature increased from 1.01×10^{-7} S/cm for the sample PVA90 to 4.87×10^{-6} S/cm for the sample PVA60 by increasing the contents of NaTf from 10 to 40 wt% as shown in Fig. 1. This demonstrates that the higher contents of NaTf salt significantly boost the ionic conductivity by providing more mobile ions [19]. By using 50 wt% of NaTf salt, free standing films could not be obtained due to brittleness resulting from the higher contents of salt. Therefore, sample

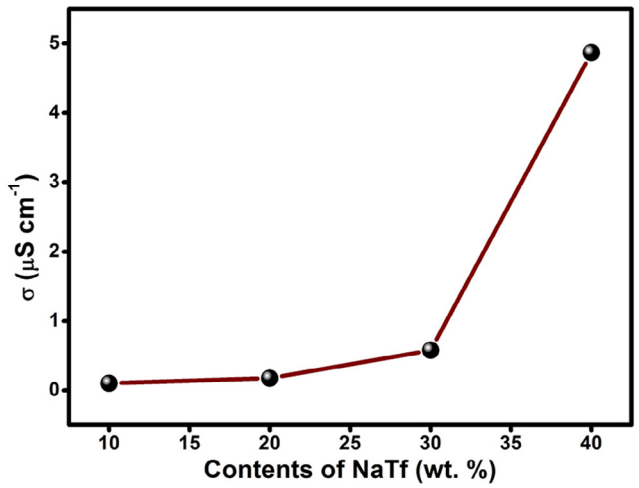

Fig. 1. The ionic conductivity of ionic liquid-free SPE at ambient temperature.

PVA60 with 40 wt% NaTf salt was chosen as optimized liquid-free SPE film.

Fig. 2 depicts the ionic conductivity of PVA-40 SPE incorporated with different contents of BmImBr ionic liquid at ambient temperature. The ionic conductivity increased from 4.87×10^{-6} to 2.31×10^{-3} S/cm with the incorporation of 50 wt% of BmImBr into the SPE sample (IL-0.5). The enhancement in the ionic conductivity is due to the strong plasticizing effect of ionic liquid that works to soften the polymer backbone thus makes the polymer more flexible for more ion transportation [20]. The ionic liquid weakens the transient coordinative bonds of the molecules and makes polymer electrolyte more amorphous. In comparison to crystalline structure, amorphous structure allows faster mobility of charge carriers [21]. Another property of ionic liquid is high dielectric constant which promotes charge carrier concentration [22]. This is due to ion separation and high dielectric constant which prevent ion aggregations as well as formation of ion clusters. However, with addition of 60 wt% BmImBr as seen in sample IL-0.6, the ionic conductivity decreased abruptly. The SPE films were not be able to accept more ions from the ionic liquid at this stage and this causes the excess ion to aggregate and neutral ion pair formation which lead to disrupt the ionic transportation [23].

The ion conduction mechanism of the SPE films was proposed as follows: The imidazolium cation ($BmIm^+$) and bromide (Br^-) anions start to separate from the ionic liquid transitory partial bonding [19]. Then, the hydrogen at C2-position of the mobile $BmIm^+$ de-protonated

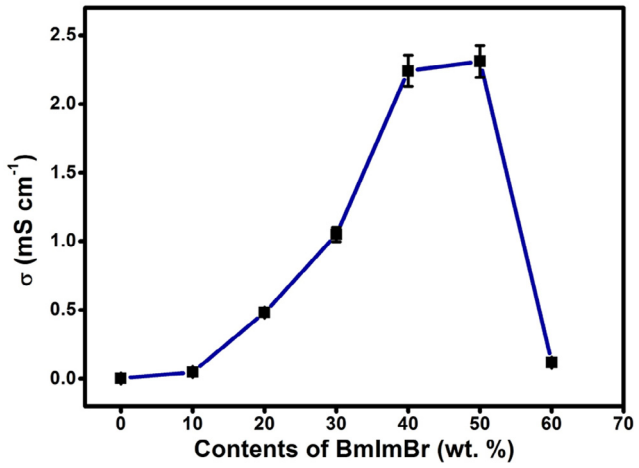

Fig. 2. The ionic conductivity of SPEs added with BmImBr ionic liquid at ambient temperature.

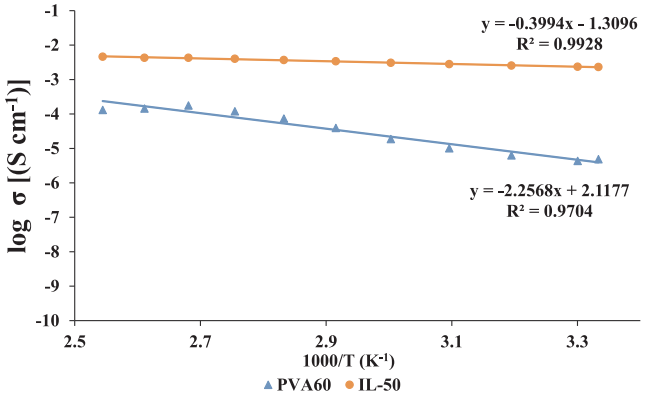

Fig. 3. Temperature dependence ionic conductivity for SPEs with (IL-0.5) and without (PVA60) the addition of BmImBr ionic liquid.

and formed a stabilized carbene. Carbocation in the imidazolium ring occurred when carbene reacts with hydrogen in hydroxyl group of PVA. Early detached bromide from ionic liquid and triflate anions from the salt would had combine with the carbocation and caused the hydrogen bond between the imidazolium cation and side chain of PVA to break. Lack of electron in the oxygen anions receive the electron from the loosely bonded sodium cations or from imidazolium cations. Hence, the ion transport mechanism takes place when the coordination bond is formed between the ions of sodium salt and negatively charged oxygen, which results in the formation of hydroxyl group through hydrogen bonding. In contrast, bromide or/and triflate anions attract the electron from hydrogen and the hydrogen turns into anions as it leaves the hydroxyl group [24].

3.2. Temperature dependence ionic conductivity analysis

The temperature dependence ionic conductivity analysis was conducted to determine the mechanism of ion transportation in ionic liquid-free SPE and ionic liquid-added SPE. The results have been plotted in Fig. 3 where the trend shows that the ionic conductivity increases with temperature. The well-fitted ionic conductivity with the trend line gives the regression value, (R^2) close to unity. Therefore, SPE films are said to obey Arrhenius theory. Below is the relationship of ionic conductivity and temperature in Arrhenius theory [25]:

$$\sigma = A\ exp(-E_a/kT) \quad (2)$$

where A is a constant and proportional to the amount of charge carriers, E_a is activation energy, k is the Boltzmann constant and T is temperature in Kelvin. Activation energy is also known as the minimum energy required by the charge carriers for the conduction. The activation energy of the ionic liquid-free and ionic liquid-based polymer electrolytes is determined and tabulated in Table 3.

According to Arrhenius theory, the mobile ions inside SPE films move inside the polymer matrix via ion hopping mechanism. The hydrogen from the hydroxyl (OH) group in PVA is initially hydrolyzed by forming hydrogen bonding with the water. Sodium triflate is then dissociated into sodium cations and triflate anions (which are known as charge carriers) when the salt is dissolved into water. Thus, the sodium cations would form weak diploe-dipole interaction with the electron withdrawing group, oxygen in the hydroxyl (OH) group of PVA. The charge carriers vibrate vigorously with increased kinetic energy once

Table 3
The activation energy obtained from the Arrhenius plots.

Designation of polymer electrolytes	Activation energy, Ea (meV)
PVA60	448
IL-50	79

being heated. Therefore, the coordination bonds between sodium cations and the oxygen could be broken easily. Hence, the sodium cations would hop from its original site to an empty neighboring site and this produces the ionic conduction.

Fig. 3 presents that ionic conductivity increases with increases in temperature. In fact, when temperature increases, the volume inside the polymer matrix increases and this provides more empty spaces for the mobile ions to move much freely. Kinetic energy of the ions increases at higher temperature and this allows more ions to be able to hop to another vacant site more easily. This phenomena increases the ion mobility in the SPE films and leading to the rise of the ionic conductivity [26]. Addition of ionic liquids helps in improving the ionic conductivity of polymer electrolytes as discussed in Section 3.1. This theory has been supported by the activation energy measurements. The activation energy has been reduced significantly from 448 meV to 79 meV by adding 50 wt% of ionic liquids into the polymer electrolytes. Ionic liquid-based polymer electrolyte requires lesser energy for ionic conduction. In other words, the charge carriers in the ionic liquid-based polymer electrolyte just have to overcome lesser potential barrier to diffuse, migrate or transport within the electrolyte. Therefore, higher ionic conductivity is obtained for ionic liquid-based electrolytes. This might be due to the strong plasticizing effect of ionic liquids which softens the polymer backbone. This favors the ionic conduction mechanism.

3.3. FTIR studies

Fig. 4 depicts the FTIR spectra of pure PVA, pure NaTf, pure BmImBr, PVA60 and IL-0.5. The main absorption band of the PVA was listed in Table 4 [27,28]. As for the pure NaTf, the symmetrical stretching of SO_3 was observed at 767 cm^{-1}, symmetrical stretching of CF_3 at 1083 cm^{-1}, asymmetrical stretching of SO_3 at 1176 cm^{-1} and 1258 cm^{-1} and symmetric vibration of CF_3 was found at 1234 cm^{-1}. All these peaks were found to be shifted to 761 cm^{-1}, 1032 cm^{-1}, 1172 cm^{-1}, and 1227 cm^{-1} in sample PVA60, respectively [29]

This characteristic peak of Tf anion at 1604 cm^{-1} was found to be disappeared in the spectrum of PVA60. These changes prove that the complexation of polymer and salt [33]. Meanwhile, the main absorption band of the pure BmImBr was associated with C-Br stretching at the peak of 651 cm^{-1}. This peak disappeared in IL-0.5 film indicating that the ionic liquid has fully dissociated forming BmIm cations and bromide anions. Therefore, these dissociated ions could form complexation with the PVA as suggested in earlier in Section 3.1. As seen in Fig. 4, the broad peak of the O–H stretching of PVA at 3386 cm^{-1} was observed to shift to 3319 cm^{-1} with increase in the intensity. This is an indication of the complexation, conduction of the ions and the O–H stretching of the PVA [34]. Another sharp peak which can be observed at 1237 cm^{-1} has been assigned as the C-O stretching mode of the PVA was shifted to 1244 cm^{-1} in IL-0.5 indicating that the C-O bond of the polymer matrix was interacting with the ions from the ionic liquid [35]. The sharp peak at 1093 cm^{-1} was also assigned as the C—O stretching mode of the PVA and this peak was remain unchanged after the addition of ionic liquid. However, the intensity of the peak was decreased upon incorporation of the ionic liquid. The skeletal C—H rocking mode which was found at 847 cm^{-1} of the PVA was shifted to 851 cm^{-1} with the incorporation of ionic liquid. It is also another indication of the occurrence of complexation between the ionic liquid and the polymer matrix.

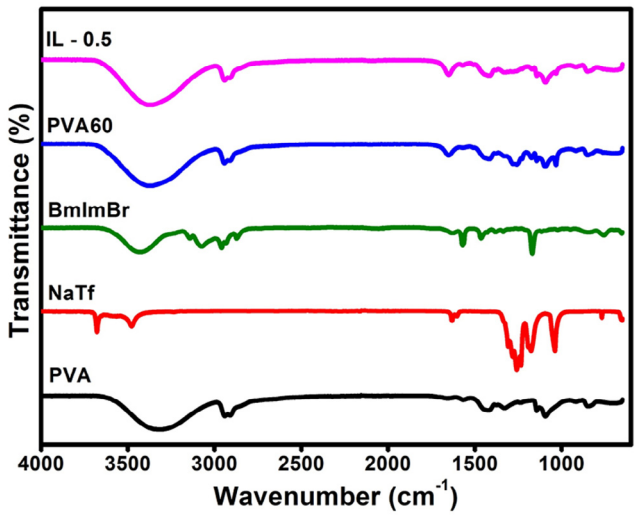

Fig. 4. The FTIR spectra of pure PVA, pure NaTf, BmImBr, PVA60 and IL-0.5 SPE.

3.4. XRD studies

The XRD patterns of PVA, pure NaTf, BmImBr, PVA60 and IL-0.5 SPE films are shown in Fig. 5. In pure PVA, sharp peaks at 2θ value of 11.5°, 41° and broad peak at 19.9° indicate the semi-crystalline nature of PVA [36,37]. Pure NaTf displayed various peaks with highly intensity at 2θ of 9.9°, 16.8°, 22.5° 26.3°, 35.6° and 40.9°, manifesting its high crystalline nature [29,38]. On the other hand, pure BmImBr spectrum shows that the ionic liquid is amorphous in nature. It is evident from the XRD patterns of PVA60 that almost all crystalline peaks of NaTf salt disappeared upon addition in PVA. This revealed the successful complexation of NaTf with PVA matrix. However, the small crystalline peaks at 19.9° in PVA60 (from PVA) is evidence of partial crystalline structure of the PVA60 complex. The amorphous nature produces better ionic diffusivity and cause high ionic conductivity which can be obtained in amorphous polymers that have a fully flexible backbone [36]. All the peaks of NaTf and PVA were completely disappeared in IL-0.5 film spectrum upon inclusion of BmImBr, which significantly increased the amorphous regions in GPE. The enhancement in the amorphousity of GPE was due to the plasticizing effects of the ionic liquid and these amorphous regions help in the movement of charges [39]. Therefore, high amorphous nature of the polymer electrolyte can facilitate the movement of ions in the polymer matrix, which can lead to increase in the ionic conductivity of the GPE [40]. Based on above argument, XRD patterns supports the ionic conductivity studies [41]. The XRD patterns are in agreement with the ionic conductivity studies where the addition of ionic liquid helped to increase the ionic conductivity due to more available mobile ions.

3.5. Thermogravimetric analysis (TGA)

The TGA curves of SPEs are shown in Fig. 6. From 25 to 125 °C, initial small weight loss of all of the pure materials and SPE samples can be observed. This is due to the removal of impurities, evaporation of absorbed moisture during the preparation of the samples [14]. The decomposition temperature of pure BmImBr and NaTf is 258 °C and 470 °C, respectively [42–44]. Meanwhile, PVA experiences two major weight loss upon until 650 °C. At 225 °C, PVA undergoes abrupt weight loss which is due to the formation of the ether cross-linkages after the evaporation of the water [45]. Besides, at this temperature, polyene could be formed also as a result of rapid chain-stripping on the polymer backbone [46]. As seen in the Fig. 6, the addition of salt and ionic liquid, the decomposition temperature at this region was increased to 227 °C and 242 °C for PVA60 and IL-0.5, respectively. This was due to the complexation between the pure materials, which has been discussed previously in XRD and FTIR studies. This complexation increases the amount of energy required to break the transient coordination and thus, increases the thermal stability at this region. On the other hand, another weight loss can be seen in IL-0.5 SPE films in the range of 290 °C–340 °C. This is attributed to the decomposition of the BmImBr [44]. It was observed that higher temperature was needed in order to break down the BmImBr inside the SPE samples. This is due to the

Table 4
The main absorption bands of pure PVA.

IR absorption bands	Wavenumbers (cm^{-1})	References
O—H stretching mode	3386	[30]
Symmetical C—H stretching mode	2942	[30]
C═O stretching mode, combination of υ(CH) and υ(CS) and C═C stretching modes	1651	[31]
CH_2 bending mode	1423	[31]
CH_2 wagging mode	1375	[31]
CH—OH bending and CH_3 in-plane deformation	1331	[32]
C—O stretching mode	1237	[32]
C—O stretching mode and O—H bending mode and CH deformation	1093	[32]
Skeletal CH rocking mode	847	[32]

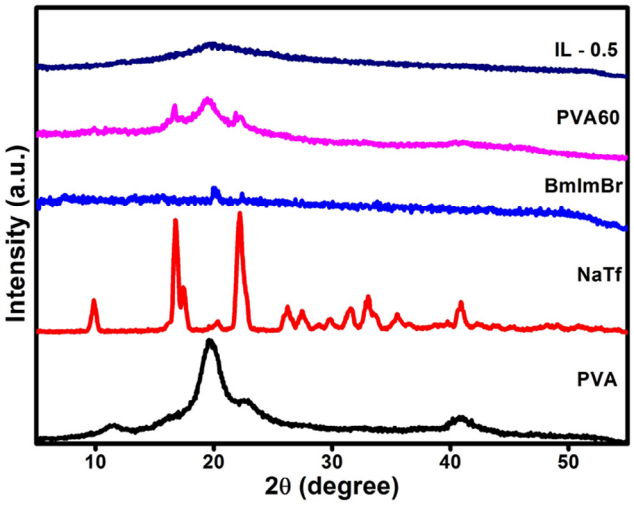

Fig. 5. XRD result of PVA, NaTf, BmImBr, PVA60 and IL-0.5 SPE.

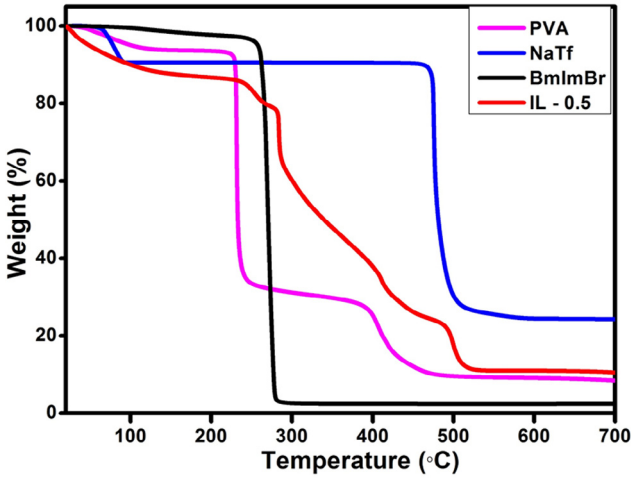

Fig. 6. Thermal stability analysis for PVA, NaTf, BmImBr and IL-0.5 SPE.

carbene which was formed from the interaction of ionic liquid with hydroxyl group of the PVA. These interaction forms a coordinated bond and therefore, more energy is needed for the BmImBr to decompose in the IL-0.5 SPE film.

The weight loss starting from 395 °C can be observed for pure PVA. This is due to further break down of the polymer backbone which can be explained by the double bond of the polyenes (that was produced previously in lower temperature eventually broken down into single bond and finally to aliphatic chains at this temperature) [47]. The decomposition temperature at this region does not vary much after the addition of the salts and ionic liquid. The degradation beyond temperature of 470 °C is most likely due to the decomposition of the NaTf salts in the SPEs. Beyond that stage, the weight of the SPE was found to be not changing and it indicated the full decomposition of the whole SPE. Sample IL-0.5 is concluded to have the best thermal properties as polymer electrolytes compared to other samples due to its first high decomposition temperature.

3.6. Electrochemical performance studies for EDLC

Cyclic voltammetry was performed in the potential window between 0 V and 1 V at different scan rates (3, 5, 10, 20, 30, 40, 50 and 100 mV/s). Fig. 7(a) and (b) depicts the CV curves of PVA60 and IL-0.5, respectively. It can be clearly seen from Fig. 7(b) that IL-0.5 SPE film possesses rectangular curve which almost symmetric about zero as compared to PVA60 which gave leaf-like shape of CV curve (shown in

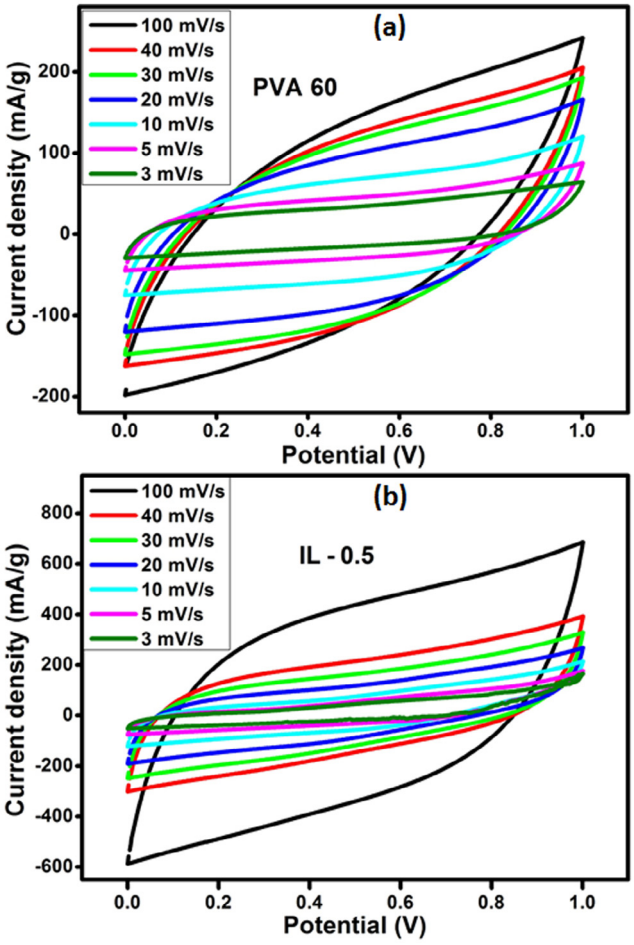

Fig. 7. CV curves of supercapacitor cell based on for (a) PVA60 SPE (i) and (b) IL-0.5 SPE at various scan rate.

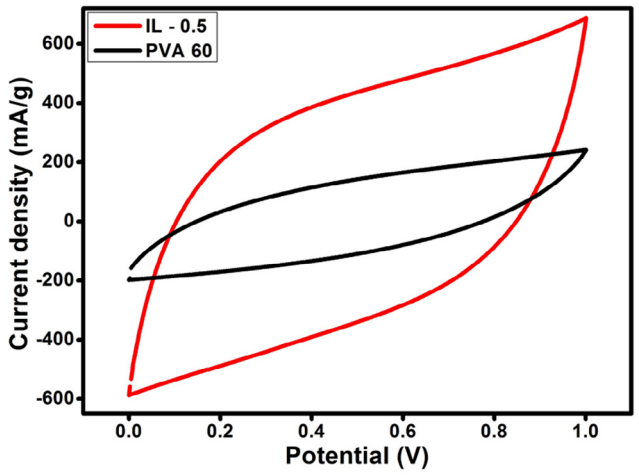

Fig. 8. CV curve of PVA60 and IL-0.5 SPE based supercapacitor at scan rate of 100 mV/s.

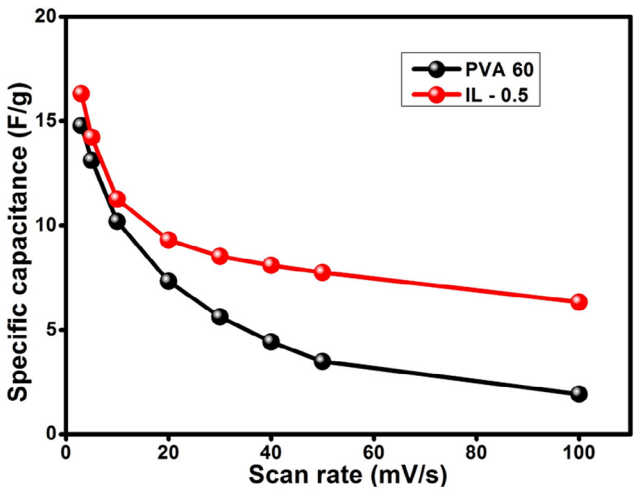

Fig. 9. Specific capacitance of PVA60 and IL-0.5 SPE at various scan rate.

Fig. 7(a)). The symmetric and rectangular CV curve is the indication of excellent capacitive behavior of IL-0.5 SPE film. In addition to this, the IL-0.5 SPE based supercapacitor maintained its rectangular shaped CV curve at higher scan rate of 100 mV/s compared to PVA60, which means that IL-0.5 SPE is highly stable and possess good rate capability.

The comparison of CV curve at 100 mV/s for PVA60 and IL-0.5 SPE based supercapacitor is displayed in Fig. 8. Wider area under the CV loop for IL-0.5 based supercapacitor compared to PVA60 SPE based supercapacitor is clear indication of superior capacitive behavior of IL-0.5 SPE film. The specific capacitance, C_{sp} was calculated using the formula [47]:

$$C_{Sp} = \frac{1}{\upsilon m V} \int I \times t \tag{3}$$

where, $\int I \times t$ is the area of the curve, m is the mass of active material on both electrodes, v is the scan rate and V is the potential window. The specific capacitance of the IL-0.5 and PVA60 SPE based supercapacitors is found to be 16.32 Fg^{-1} and 14.78 Fg^{-1}, respectively. IL-0.5 SPE based supercapacitor displayed enhanced performance compared to supercapacitor using PVA60. The specific capacitance values are comparable to the reported specific capacitance values by SPE based EDLC in the literature (Table 5)

The enhancement in specific capacitance of IL based cell was owing to the availability of mobile ions provided by the IL. This high ion contents provides more charge accumulation at the electrode–electrolyte boundary, hence, improved the energy storage.

From Fig. 9 it can be seen that specific capacitance PVA60 SPE based supercapacitor dropped very fast compared to IL-0.5 SPE based supercapacitor which reveals the poor rate capability of the PVA60 SPE.

The galvanostatic charge/discharge (GCD) curves of IL-0.5 SPE based supercapacitor are show in Fig. 10(a). The capacitive nature of the supercapacitor fabricated by using IL-0.5 SPE film was proved by the symmetrical charge discharge curves (Fig. 10(a)). The supercapacitor started to charge at 0.23 V instead of 0 V due to the internal resistance of the supercapacitor and drop in the initial part of the discharge curve (also known as ohmic loss) was also due to the internal resistance of electrochemical capacitors which comes from the resistances between electrode and electrolyte, such as charge transfer resistance and bulk resistance of polymer electrolyte [1,15].

The ohmic loss tends to increase with the number of charge/discharge cycles due to the depletion of polymer electrolyte which was caused by the decreasing of mobile ions due to their migration and accumulation in the electrical double layer [25]. However, as seen in Fig. 10(a), the ohmic loss of the supercapacitor with IL-0.5 SPE only increased from 0.281 V to 0.284 V proving that the IL-0.5 SPE is suitable for EDLC application. Fig. 10(b) shows the galvanostatic discharge curves of the assembled supercapacitor cells at current densities of 125, 150, 175, and 200 mA/g at room temperature for the SPE sample with and without BmImBr. It can be seen that the addition of ionic liquid increases the discharging time of the EDLC. This affirms that the supercapacitor with IL-0.5 SPE shows better capability of charge storage compared to supercapacitor using SPE without ionic liquid.

The EIS measurements (Nyquist plot) were recorded for both (with and without ionic liquid) supercapacitor cells in the range from 0.01 to 1 MHz, which are displayed in Fig. 11. Both samples showed small semicircle at low frequency region and formed inclined spike at high frequency region. The first intersecting point of Nyquist plot to the real axis at low frequency is known as equivalence series resistance, which originates due to the internal resistance, resistance of connecting wire and its connections [52]. The second intersecting of Nyquist plot (R_{ct}) to the real axis is due to the charge transfer resistance between electrode and electrolyte. The inclined line at high frequency region arises due to the capacitive behavior of the device due to adsorption and intercalation charges [8]. In IL-0.5 SPE supercapacitor, spike formed is higher than in PVA60 indicates large charge accumulation at the electrode-electrolyte boundary which is due to presence of ions from ionic liquid. The charge transfer resistance (R_{ct}) of the SPEs were determined from diameter of the semicircle found at the high frequency of the impedance plot [53]. The R_{ct} value of the supercapacitor cells were 21 Ω and 16 Ω using PVA60 SPE and IL-0.5 SPE, respectively. The low resistance of IL-0.5 SPE based supercapacitor is attributed to the high conductivity and sticky nature of the BmImBr that has been added into the IL-0.5 SPE. The improved conductivity of IL-0.5 SPE based supercapacitor compared to its counterpart is in well agreement of conductivity studies and the reported results in the literature [54,55]. It improved the contact between the electrolyte-electrode, decreasing

Table 5
Performance comparison of IL-0.5 SPE based EDLC with reported SPE based EDLC in the literature.

	Electrolyte	Scan rate (mV/s)	Specific Capacitance (F/g)	Reference
1	PAA-LiTFSI-TiO_2	10	28.5	[16]
2	PMMA-$Mg(CF_3SO_3)_2$)	5	27	[48]
3	HEC-$MgTf_2$-EMIMTf	5	25	[8]
4	PVA-$LiClO_4$	10	12.5	[49]
5	Corn starch-$LiClO_4$-SiO_2	10	8.7	[50]
6	PVA-ammonium acetate-BmImTf	10	2	[51]
7	PVA- NaTf- BmImBr	3	16.3	Current work

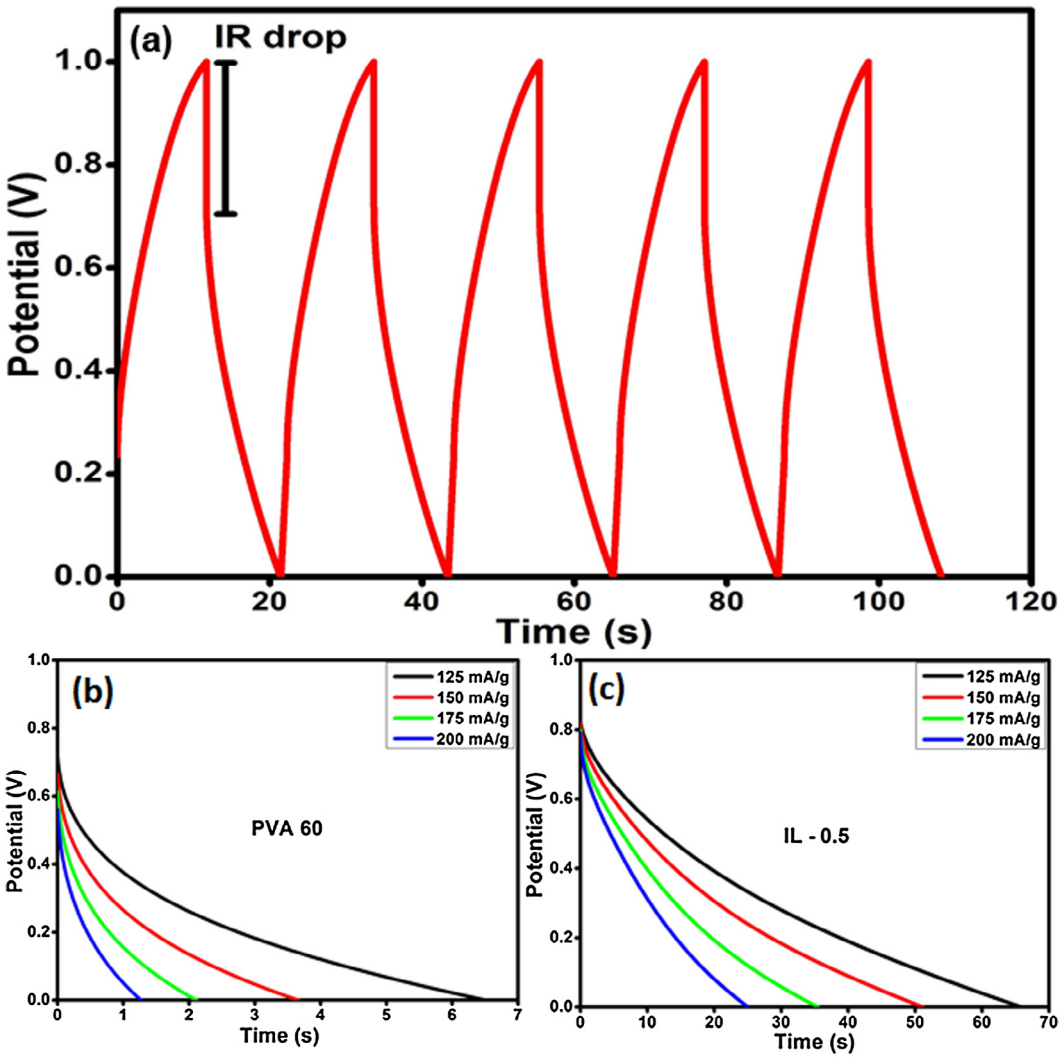

Fig. 10. (a) GCD curves over first 5 cycles and (b) galvanostatic discharge curves for EDLCs fabricated using PVA60 and IL-0.5 SPE at various current densities.

resistance and thus, reducing the R_{ct} of the supercapacitor.

Long-term cycling stability test is a key factor to evaluate the performance of SPE for practical applications. The long-term cycling performance of IL-0.5 SPE supercapacitor over 1000 cycles was conducted by repeating the charge/discharge test at a current density of 200 mA/g and the results are shown in Fig. 12. Initially, the specific capacitance was stable up to 350 cycles. With further charge/discharge cycling, specific capacitance decreased slowly. After 1000 cycles, the capacitive retention dropped by 30%. The coulombic efficiency of supercapacitor is an important parameter to evaluate the reliability of EDLC. Therefore, coulombic efficiency (η) of IL-0.5 SPE based supercapacitor was calculated using the following equation:

$$\eta = \frac{t_d}{t_c} \times 100\% \tag{4}$$

where t_c and t_d represents the charge and discharge time, respectively. The coulombic efficiency of EDLC over 1000 cycles are depicted in Fig. 12.

The supercapacitor with IL-0.5 SPE exhibits coulombic efficiency that remains at 77% to 87% over 1000 cycle. The supercapacitor cell remains stable above until 150th cycle and then there was a slight drop until 1000th cycle and reach to the minimum value of 81%. This inferred the electrode and electrolyte has intimate contact with each other [56].

4. Conclusion

A free standing PVA (incorporated with NaTf salt and BmImBr ionic liquid) based SPE film was prepared using solution casting method. The performance of SPEs with and without ionic liquid was compared for supercapacitor application. The conductivity results revealed that addition of 50 wt% BmImBr ionic liquid in PVA60 improved the ionic conductivity at room temperature from 4.87×10^{-6} S/cm to 2.31×10^{-3} S/cm. The temperature dependence studies depicted that the prepared SPEs obey Arrhenius theory. FTIR and XRD studies were done and the formation of complexes among the host polymer, salt and ionic liquid was analyzed. The IL-0.5 SPE was found to be thermally stable up to at least 236 °C. The highly conductive ionic liquid-based SPE (IL-0.5) and ionic liquid-free SPE (PVA60) were used to fabricate supercapacitor cells. The maximum specific capacitance of 16.32F g^{-1} was found by IL-0.5 SPE supercapacitor at 3 mV/s. The GCD and EIS curves indicated that was IL-0.5 SPE supercapacitor suitable for energy storage application compared to PVA60 SPE based supercapacitor cell.

Declaration of Competing Interest

The authors declare that they have no known competing financial interests or personal relationships that could have appeared to influence the work reported in this paper.

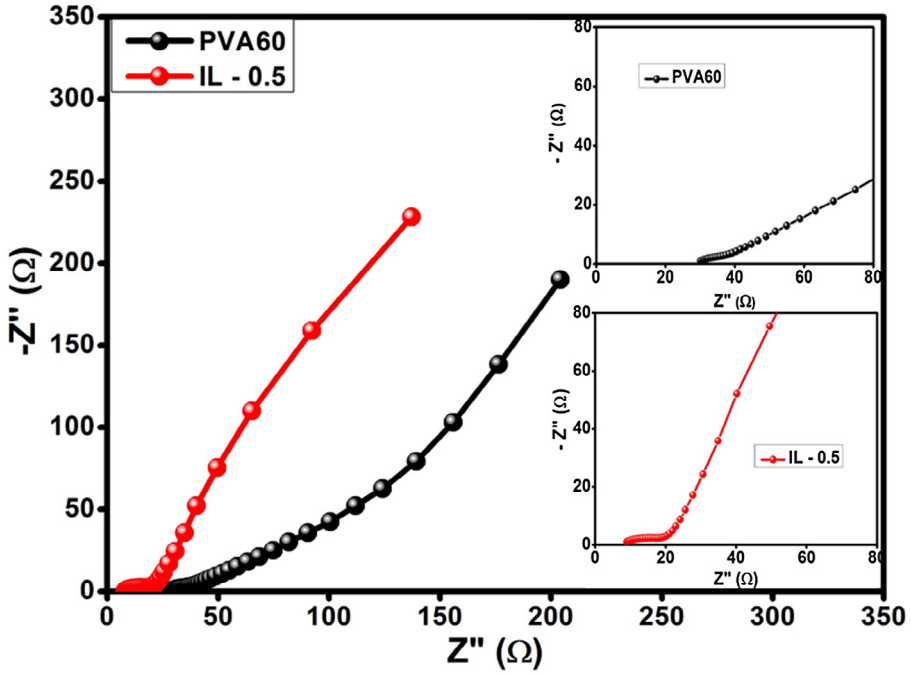

Fig. 11. Nyquist Plots for EDLCs fabricated by using PVA60 and IL-0.5 SPE.

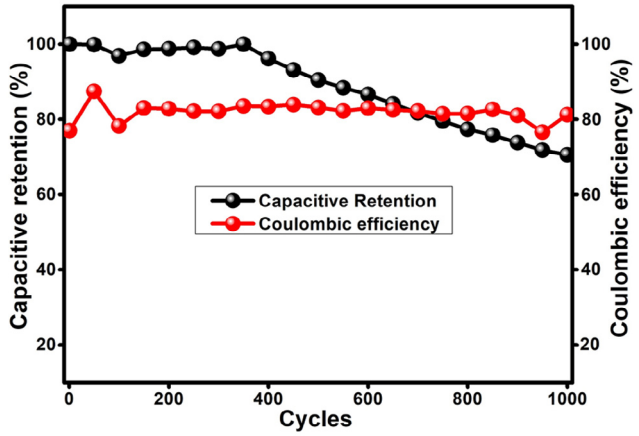

Fig. 12. The variation of specific capacitance as a function of cycle number from 5th to 1500th for sample IL-0.5 SPE.

Acknowledgements

This work is financially supported by Fundamental Research Grant Scheme (FRGS) from Ministry of Education, Malaysia (FP062-2018A). The authors would like to thank Collaborative Research in Engineering, Science & Technology Center (CREST) for their continuous support in this research (PV027-2018). A special thank you to ECLIMO SDN BHD as well.

References

[1] M.Y. Chong, et al., Comparison of the performance of copper oxide and yttrium oxide nanoparticle based hydroxylethyl cellulose electrolytes for supercapacitors, J. Appl. Polym. Sci. 134 (13) (2017).
[2] K. Rajammal, et al., Enhanced electrochemical properties of ZnO-coated LiMnPO4 cathode materials for lithium ion batteries, Ionics 22 (9) (2016) 1551–1556.
[3] M.Z. Iqbal, et al., Ultrasonication-assisted synthesis of novel strontium based mixed phase structures for supercapattery devices, Ultrason. Sonochem. (2019) 104736.
[4] A. Numan, et al., Sonochemical synthesis of nanostructured nickel hydroxide as an electrode material for improved electrochemical energy storage application, Progress Natural Sci.: Mater. Int. 27 (4) (2017) 416–423.
[5] N. Duraisamy, et al., Development of asymmetric device using Co 3 (PO 4) 2 as a positive electrode for energy storage application, J. Mater. Sci.: Mater. Electron. 30 (8) (2019) 7435–7446.
[6] I. Heng, et al., Low-temperature synthesis of TiO2 nanocrystals for high performance electrochemical supercapacitors, Ceram. Int. 45 (4) (2019) 4990–5000.
[7] Y. Sudhakar, M. Selvakumar, D.K. Bhat, Tubular array, dielectric, conductivity and electrochemical properties of biodegradable gel polymer electrolyte, Mater. Sci. Eng., B 180 (2014) 12–19.
[8] M.Y. Chong, et al., Enhancing the performance of green solid-state electric double-layer capacitor incorporated with fumed silica nanoparticles, J. Phys. Chem. Solids 117 (2018) 194–203.
[9] M.L. Verma, M. Minakshi, N.K. Singh, Synthesis and characterization of solid polymer electrolyte based on activated carbon for solid state capacitor, Electrochim. Acta 137 (2014) 497–503.
[10] Y. Zhu, et al., A new single-ion polymer electrolyte based on polyvinyl alcohol for lithium ion batteries, Electrochim. Acta 87 (2013) 113–118.
[11] M. Aziz, et al., PVA based gel polymer electrolytes with mixed iodide salts (K+ I− and Bu 4 N+ I−) for dye-sensitized solar cell application, Electrochim. Acta 182 (2015) 217–223.
[12] L. Jia, et al., Electrochemical deposition semiconductor ZnSe on a new substrate CNTs/PVA and its photoelectrical properties, Electrochim. Acta 107 (2013) 71–77.
[13] D.J. Kim, et al., An aqueous sodium ion hybrid battery incorporating an organic compound and a Prussian blue derivative, Adv. Energy Mat. 4 (12) (2014).
[14] C.-W. Liew, S. Ramesh, A. Arof, Characterization of ionic liquid added poly (vinyl alcohol)-based proton conducting polymer electrolytes and electrochemical studies on the supercapacitors, Int. J. Hydrogen Energy 40 (1) (2015) 852–862.
[15] N. Fattah, et al., An approach to solid-state electrical double layer capacitors fabricated with graphene oxide-doped, ionic liquid-based solid copolymer electrolytes, Materials 9 (6) (2016) 450.
[16] C.-W. Liew, et al., Poly (acrylic acid)–based hybrid inorganic-organic electrolytes membrane for electrical double layer capacitors application, Polymers 8 (5) (2016) 179.
[17] R. Rajendran, et al., Dimensionally integrated nanoarchitectonics for a novel composite from 0D, 1D, and 2D nanomaterials: RGO/CNT/CeO 2 ternary nanocomposites with electrochemical performance, J. Mater. Chem. A 2 (43) (2014) 18480–18487.
[18] R. Rajendran, et al., Composite nanoarchitectonics for ternary systems of reduced graphene oxide/carbon nanotubes/nickel oxide with enhanced electrochemical capacitor performance, J. Inorg. Organomet. Polym Mater. 25 (2) (2015) 267–274.
[19] Y. Yang, W. Wang, A new polymer electrolyte for solid-state quantum dot sensitized solar cells, J. Power Sources 285 (2015) 70–75.
[20] C.-W. Liew, S. Ramesh, Electrical, structural, thermal and electrochemical properties of corn starch-based biopolymer electrolytes, Carbohydr. Polym. 124 (2015) 222–228.
[21] A.S. Shaplov, R. Marcilla, D. Mecerreyes, Recent advances in innovative polymer electrolytes based on poly (ionic liquid) s, Electrochim. Acta 175 (2015) 18–34.
[22] Y. Kumar, G. Pandey, S. Hashmi, Gel polymer electrolyte based electrical double layer capacitors: comparative study with multiwalled carbon nanotubes and activated carbon electrodes, J. Phys. Chem. C 116 (50) (2012) 26118–26127.
[23] Y. Ye, et al., Enhanced ion transport in polymer–ionic liquid electrolytes containing

ionic liquid-functionalized nanostructured carbon materials, Carbon 86 (2015) 86–97.
[24] J.P. Canal, et al., From the reactivity of N-heterocyclic carbenes to new chemistry in ionic liquids, Chem. Commun. 17 (2006) 1809–1818.
[25] A. Kumar, et al., Li-ion transport, structural and thermal studies on lithium triflate and barium titanate incorporated poly (vinylidene fluoride-co-hexafluoropropene) based polymer electrolyte, Solid State Ionics 289 (2016) 150–158.
[26] C.-W. Liew, et al., Electrical and structural studies of ionic liquid-based poly (vinyl alcohol) proton conductors, J. Non-Cryst. Solids 425 (2015) 163–172.
[27] G. Hirankumar, et al., AC impedance studies on proton conducting polymer electrolyte complexes (PVA+ CH 3 COONH 4), Ionics 10 (1) (2004) 135–138.
[28] M. Hema, et al., FTIR, XRD and ac impedance spectroscopic study on PVA based polymer electrolyte doped with NH 4 X (X= Cl, Br, I), J. Non-Cryst. Solids 355 (2) (2009) 84–90.
[29] S.B. Aziz, Z.H.Z. Abidin, Electrical conduction mechanism in solid polymer electrolytes: new concepts to arrhenius equation, J. Soft Matter 2013 (2013).
[30] A. Kharazmi, et al., Structural, optical, opto-thermal and thermal properties of ZnS–PVA nanofluids synthesized through a radiolytic approach, Beilstein J. Nanotechnol. 6 (2015) 529.
[31] N. Bhat, et al., Effect of γ-radiation on the structure and morphology of polyvinyl alcohol films, Nucl. Instrum. Methods Phys. Res., Sect. B 237 (3–4) (2005) 585–592.
[32] I. Omkaram, R.S. Chakradhar, J.L. Rao, EPR, optical, infrared and Raman studies of VO2+ ions in polyvinylalcohol films, Physica B 388 (1–2) (2007) 318–325.
[33] S. Rajendran, M. Sivakumar, R. Subadevi, Li-ion conduction of plasticized PVA solid polymer electrolytes complexed with various lithium salts, Solid State Ionics 167 (3–4) (2004) 335–339.
[34] N. Kakati, et al., An approach of balancing the ionic conductivity and mechanical properties of PVA based nanocomposite membrane for DMFC by various cross-linking agents with ionic liquid, Int. J. Hydrogen Energy 40 (22) (2015) 7114–7123.
[35] A. Awadhia, S. Agrawal, Structural, thermal and electrical characterizations of PVA: DMSO: NH 4 SCN gel electrolytes, Solid State Ionics 178 (13) (2007) 951–958.
[36] O.W. Guirguis, M.T. Moselhey, Thermal and structural studies of poly (vinyl alcohol) and hydroxypropyl cellulose blends, Natural Science 4 (1) (2012) 57.
[37] M. Muthuvinayagam, C. Gopinathan, Characterization of proton conducting polymer blend electrolytes based on PVdF-PVA, Polymer 68 (2015) 122–130.
[38] S.B. Aziz, et al., Effect of high salt concentration (HSC) on structural, morphological, and electrical characteristics of chitosan based solid polymer electrolytes, Polymers 9 (6) (2017) 187.
[39] M.Y. Chong, et al., Effects of ionic liquid on the hydroxylpropylmethyl cellulose (HPMC) solid polymer electrolyte, Ionics 22 (12) (2016) 2421–2430.
[40] A.N. Mee Yoke Chong, Chiam-Wen Liew, K. Ramesh, S. Ramesh, Comparison of the performance of copper oxide and yttrium oxide nanoparticle based hydroxylethyl cellulose electrolytes for supercapacitors, J. Appl. Polymer Sci. (2016).
[41] R.A. Sanders, et al., A spectroscopic and conductivity comparison study of linear poly (N-methylethylenimine) with lithium triflate and sodium triflate, Electrochim. Acta 48 (14) (2003) 2247–2253.
[42] P.A.B. Ranjana, et al., Enhancement of Na+ ion conduction in polymer blend electrolyte P (VdF-HFP)–PMMA-NaTf by the inclusion of EC, J. Polym. Res. 26 (2) (2019) 38.
[43] S. Hashmi, et al., Ionic liquid-based sodium ion-conducting composite gel polymer electrolytes: effect of active and passive fillers, J. Solid State Electrochem. 20 (10) (2016) 2817–2826.
[44] Y. Cao, T. Mu, Comprehensive investigation on the thermal stability of 66 ionic liquids by thermogravimetric analysis, Ind. Eng. Chem. Res. 53 (20) (2014) 8651–8664.
[45] S. Kayal, R. Ramanujan, Doxorubicin loaded PVA coated iron oxide nanoparticles for targeted drug delivery, Mater. Sci. Eng., C 30 (3) (2010) 484–490.
[46] A. Das, A.K. Thakur, K. Kumar, Evidence of low temperature relaxation and hopping in ion conducting polymer blend, Solid State Ionics 262 (2014) 815–820.
[47] I. Stoševski, et al., Improved Poly (vinyl alcohol)(PVA) based matrix as a potential solid electrolyte for electrochemical energy conversion devices, obtained by gamma irradiation, Energy 90 (2015) 595–604.
[48] S. Asmara, et al., Preparation and characterization of magnesium ion gel polymer electrolytes for application in electrical double layer capacitors, Electrochim. Acta 57 (2011) 91–97.
[49] C.-S. Lim, et al., Capacitive behavior studies on electrical double layer capacitor using poly (vinyl alcohol)–lithium perchlorate based polymer electrolyte incorporated with TiO2, Mater. Chem. Phys. 143 (2) (2014) 661–667.
[50] K. Teoh, et al., Electric double-layer capacitors with corn starch-based biopolymer electrolytes incorporating silica as filler, Ionics 21 (7) (2015) 2061–2068.
[51] S. Agrawal, et al., Studies on multiferroic oxide-doped PVA-based nanocomposite gel polymer electrolyte system for electrochemical device application, Ionics (2018) 1–10.
[52] A. Numan, et al., Binary nanocomposite of Co3O4 nanocubes supported on carbon matrix for supercapattery, 2018.
[53] J. Iqbal, et al., High performance supercapattery incorporating ternary nanocomposite of multiwalled carbon nanotubes decorated with Co3O4 nanograins and silver nanoparticles as electrode material, Electrochim. Acta 278 (2018) 72–82.
[54] B.-S. Cho, J. Choi, K.-Y. Kim, Preparation and properties of solid polymer electrolyte based on imidazolium-based ionic liquids for structural capacitors, Fibers Polym. 18 (8) (2017) 1452–1458.
[55] J. Chew, et al., Performance studies of ZnO and multi walled carbon nanotubes-based counter electrodes with gel polymer electrolyte for dye-sensitized solar cell, Mater. Sci. Semicond. Process. 83 (2018) 144–149.
[56] C.-S. Lim, et al., Capacitive behavior studies on electrical double layer capacitor using poly (vinyl alcohol)–lithium perchlorate based polymer electrolyte incorporated with TiO 2, Mater. Chem. Phys. 143 (2) (2014) 661–667.